

Control of Free Radical Reactivity in Photopolymerization of Acrylates

*Patrick Kramer**, Rutgers University, New Brunswick, NJ

Leonard Davis, Sun Chemical Corporation, Carlstadt, NJ

Richard Jones†, Sun Chemical Corporation, Carlstadt, NJ

Abstract

In practical use, it is the rate of cross-linked network formation that is of most interest in the free radical curing of acrylates. One of the simplest indicators of the vitrification point is the sharp rise in MEK double rubs (MEKR) that occurs as a function of radiation dose applied. It is well-known that oxygen inhibition and radical-radical recombination limit efficiency, delaying the onset of glassy network formation to higher dose or longer exposure time. This paper explores means to alter the reactivity of the intermediate free radicals, in one case by chain transfer to thiol and in another by complexation with stable nitroxide radicals, thereby altering the population of chain-carrying species to favor longer-lived radicals or radical precursors which by their nature are less affected by the normal termination processes. By chain transfer formation of thiyl radicals, a simple titration of reactive radicals is possible as observed by detection of the point of maximum MEKR as a function of dose for different starting thiol concentrations. By this means, we can demonstrate that approximately 7 times more radicals are created in a typical UV cure formula following 600 mJ/cm² exposure than are created in an EB cure formula using the same monomer following 30 kGy exposure. At low concentrations of organic nitroxides, a surprising decrease in radiation dose at the vitrification point is observed, paired with an increase in ultimate rub resistance. This optimal concentration depends strongly on nitroxide structure, but in all cases it occurs at nitroxide concentrations much smaller than the estimated free radical concentration at the point of cure. Both observations are consistent with a colloidal model of gelation where first-formed cure domains are cemented together in a slower second step. Finally, we show that latent cure is accentuated by these longer lived radicals and oxidation products formed from them, allowing a post heat to significantly advance cure by re-initiation of free radicals.

*Presenter and principal author

†To whom correspondence should be addressed: richard.jones@sunchemical.com

1 Introduction

The ultraviolet (UV) and electron beam (EB) polymerization of acrylated materials proceeds by a radical addition mechanism. During a photocure event, a large number of highly reactive radical species are produced with a short, intense exposure to radiation.¹ The production and consumption of these radical species is typically organized into four major steps: initiation, propagation, chain transfer, and termination, as illustrated in the following.^{2,3}

Initiation depends on the formation of free radical species. This step generally begins with the fragmentation of a photoinitiator (UV) or acrylated monomer (EB) upon exposure to radiation:



Included in the initiation step is the addition of an initiating radical $I\cdot$ to a monomer molecule:



It is our convention that $I\cdot$ is an initiating radical with correct electronic structure to efficiently add to the monomer, while $A\cdot$ is a radical species with lower probability to initiate chain growth.²⁻⁶ The group X denotes the remainder of the monomer molecule. As this paper focuses on crosslinking systems, X generally contains multiple acrylate groups.

Propagation occurs when the product of a previous radical addition, $R\cdot$, encounters and adds to an unsaturated group:



A radical species of greater molecular weight is produced, which may continue in further addition reactions.

Alternatively, when a radical species $R^1\cdot$ approaches a growing or terminated chain R^2-H with an accessible hydrogen, abstraction of this atom may occur:



This chain transfer event results in the termination of $R^1\cdot$'s growth, but $R^2\cdot$ may now act as a propagating species.

Radical species are eliminated from propagation by a number of rapid termination reactions. As carbon-centered radicals are highly reactive, their combination with other radicals to produce a closed shell species is favored and this reaction is considered irreversible on the timescale of radiation curing. One form of termination pathway is radical-radical recombination:



where $R^1\cdot$ and $R^2\cdot$ are growing radical chains or initiating radicals. A second type of termination is the reaction of a propagating radical with triplet oxygen to form a peroxy radical species:



The alkyl peroxy radical does not undergo further addition to monomer;⁷ oxygen inhibition, the common name for this termination reaction, is a major drawback to photopolymerizations conducted in air.^{8,9}

The rate of double bond conversion (reaction (3)) is of primary importance only in the early stages of cure, prior to gelation. After gelation occurs, great differences in mechanical properties can be evident with only minor differences in overall conversion.¹⁰ Thus, instead of monitoring cure kinetics in terms of conversion, we study the final network properties as a function of total exposure to radiation. The strength of a radiation-cured acrylate polymer film depends on the rate of vitrification, so better cure kinetics leads to a stronger polymer network at lower exposure.

The evolution of this network is hindered by termination reactions such as oxygen inhibition and radical-radical recombination. If a significant number of the propagating radical species can be protected from such unproductive termination reactions, favorable network properties can develop with shorter irradiation times or with less input of energy. Through more efficient use of initiating radicals, curing at faster web speeds, lower lamp power, or with less inerting can lead to the same mechanical properties expected or even improved properties.

In this work, we investigate several methods of controlling photopolymerization by changing the nature of the propagating radical. The strategies employed are: chain transfer to produce thiyl radicals from carbon radicals using multifunctional thiols, reversible complexation of carbon radicals by stable nitroxide radicals, and thermal post cure of a radiation cured system.

2 Experimental

2.1 Materials

All coating solutions were based on the monomer, ethoxylated trimethylolpropane triacrylate (EOTMPTA, Photomer 4149, IGM Resins) (Figure 1, (a)). This monomer was used as received, without removal of inhibitor. The base stock solution solution for electron beam curing consisted of 0.5% (w/w) BYK-345 (BYK-Chemie), a proprietary leveling agent, in EOTMPTA.

To prepare the stock coating solution for UV application, 2% (w/w) of the photoinitiator, 1-[4-(2-hydroxyethoxy)phenyl]-2-hydroxy-2-methyl-1-propane-1-one (Irgacure 2959, Ciba, BASF), 15% (w/w) of a proprietary amine acrylate, CN373 (Sartomer Company, Inc.), and 0.5% (w/w) BYK-345 were added to EOTMPTA.

Thiol-containing stock solutions for UV and EB were prepared with 4 % (w/w) pentaerythritol tetra-3-mercaptopropionate (PETMP, Hampshire Chemical Corporation) (Figure 1, (b)) added to the respective base stock solution. An equal mass of EOTMPTA to the added PETMP is removed in the preparation of thiol stock solutions, so that the concentrations of other additives (photoinitiator, acrylated amine, leveling agent) do not differ from the base stock solutions. Samples with intermediate PETMP concentrations were prepared by blending the original stock solutions with thiol-containing stock solutions. The PETMP concentrations are reported as mmol PETMP per kilogram solution. All thiol-containing solutions were used for cure trials within one week of mixing.

The stable nitroxide radicals used in this work were di-*tert*-butyl nitroxide (DBuN, Aldrich), BlocBuilder RC-50 (Arkema, Inc.), and Irgastab UV 10 (Ciba, BASF); refer to Figure 1, (c-e) for the chemical structures. DBuN was obtained as a liquid sample of 90 % purity, UV 10 as a crystalline solid, and RC-50 as a 5 % solution in dibutyl maleate (DBM). Solutions of 4.5 percent DBuN and 2.5 percent UV 10, by mass, were prepared by dissolving the respective materials in dibutyl maleate (Aldrich). The base stock solution was modified to account for the presence of the plasticizer DBM in the working solutions of nitroxides: four percent by mass of the EOTMPTA

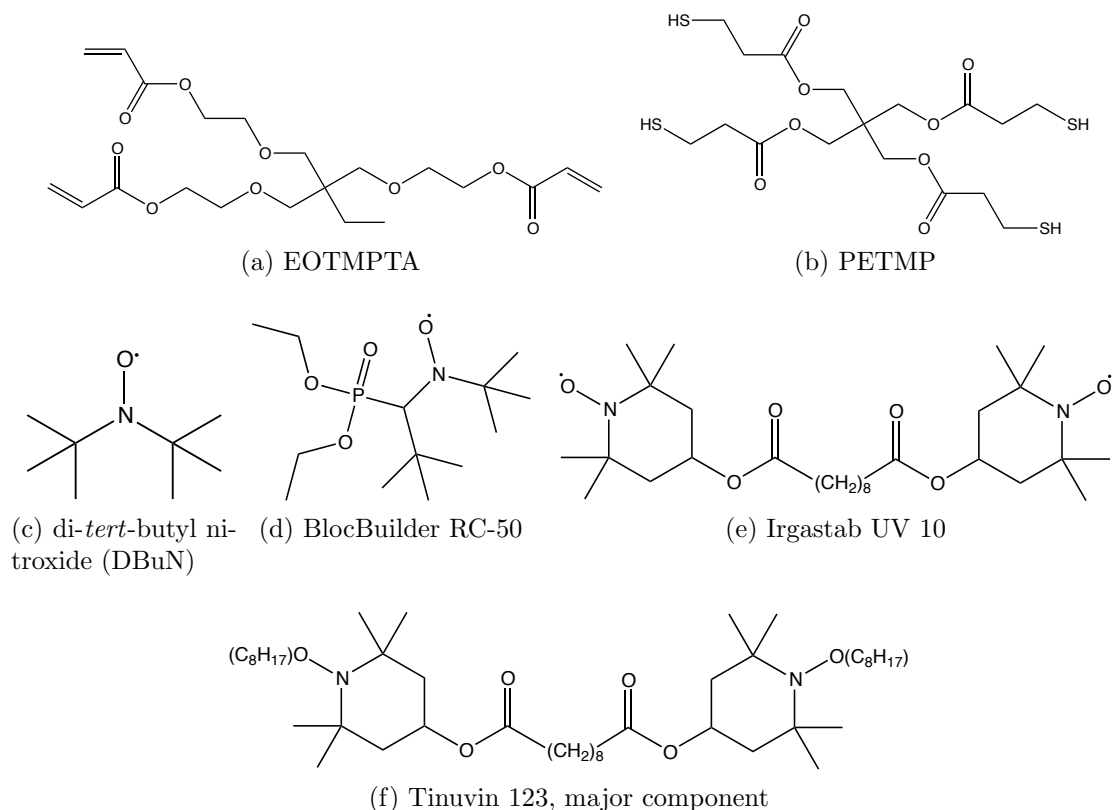


Figure 1: Structures of monomer, thiol, nitroxide, and alkoxyamine materials used in this work.

content in the previously described EB and UV base solutions was replaced by DBM to form the base solution for nitroxide investigation. Coating solutions containing the maximum concentration of nitroxide were prepared by replacing the 4 % DBM with four percent of the appropriate DBuN, RC-50, or UV 10 solution. Intermediate nitroxide concentrations were achieved by blending the 4 % DBM base solution with the 4 % nitroxide stock at appropriate ratios. The concentration of each nitroxide is reported as mmol nitroxide molecule per kilogram solution. Note that UV 10 contains two nitroxide ($\text{NO}\cdot$) groups per molecule; each mmol/kg of UV 10 represents two mmol/kg of the nitroxide group. We compare UV 10 to other materials in terms of its molecular diradical concentration since the two $\text{NO}\cdot$ groups do not necessarily act independently.

As a representative alkoxyamine (NOR) compound, we used Tinuvin 123 (Ciba, BASF). The major component of this hindered amine light stabilizer (HALS), according to the manufacturer's analysis, is the alkoxyamine product of UV 10 with two octyl groups (presumably attached in secondary positions) as shown in Figure 1, (f). Other higher molecular weight components are present, and we normalize Tinuvin 123 concentrations to the number of UV 10 mmoles per kilogram solution. The stock solutions for Tinuvin 123 evaluation were prepared similarly to those for the nitroxides. Four percent of the alkoxyamine material replaced the same mass of the solvent DBM in UV and EB stock solutions to prepare the Tinuvin 123 concentrated stock coating solution. Intermediate concentrations of the alkoxyamine were achieved by blending the Tinuvin 123 stock solutions for EB or UV with the control EB/UV solutions used for nitroxide experiments.

2.2 Methods

Solutions were applied to unsealed Leneta cards (form N2A, Leneta Company) using a US number 3 Meyer rod for a constant coating thickness.

UV curing was conducted with a single 300 watts-per-inch medium pressure mercury lamp under air. Web speed was varied and the exposure was monitored by a UV Power Puck (EIT). The recorded exposure is the sum of UVA, UVB, and UVC energy densities.

An Advanced Electron Beam (AEB) laboratory processor with nitrogen inerting was used for EB curing. For typical sample exposure, the chamber was flushed with nitrogen until oxygen concentration was below 200 ppm. To investigate the sensitivity of results to inerting level, we used short inerting times to achieve up to about 700 ppm O₂ at the time of irradiation. Cures were conducted below 200 ppm O₂ unless otherwise noted. Applied dose was varied by adjusting beam current at 100 keV, with a constant web speed of 75 fpm.

The parameter of greatest interest from a practical perspective, and the one we measured directly to characterize extent of cure, is the toughness of the final polymerized film. The technique used to ascertain cured film toughness was methyl ethyl ketone (MEK) double rubs, abbreviated MEKR henceforth. A cotton tipped swab was dipped in MEK, pressed against the film over the black (inked) portion of the Leneta card, and an up-and-down rubbing motion was performed with a standard, hard pressure against the card. The number of double rubs (one rub downward followed by another back up to the starting position) necessary to break through the film and reveal the white paper beneath the black ink, uniformly over the rubbed area, was recorded as the MEKR resistance for the film in question.

Solvent rubs in general test the resistance of a cured thin film to solvent swelling as well as physical strain from the rubbing action. A film's susceptibility to these processes decreases with the extent of crosslinking. Thus we used MEKR as a measure of the global extent of crosslinking, which develops during the final stages of cure with very small changes in double bond conversion.¹⁰

3 Cure Enhancement by Chain Transfer

Thiols are well-known chain transfer agents in radical polymerization.^{3,11,12} The chain transfer constant, or the ratio of chain transfer rate constant to propagation rate constant, for n-butyl mercaptan in styrene (a typical thiol in a monomer analogous to acrylates) is $C_S = 21$.³ That is, for a propagating radical, hydrogen abstraction to form thiyl radicals occurs twenty one times more rapidly than addition to monomer double bonds. Such speed is necessary in radiation cured polymerizations, where consumption of monomer is very rapid due to the high initial concentration of radicals.¹

By inclusion of thiol species into a formula for radiation curing, we add several reactions to the general scheme presented earlier. Let Y-SH represent a (possibly multifunctional) thiol. Any radical that comes into contact with the thiol group is likely to abstract hydrogen:



Thus, normally unproductive radicals such as A · and ROO · are replaced by thiyl radicals (Y-S ·), “soft” radical species which efficiently add to acrylate double bonds.^{13,14} Chain transfer between

carbon radicals (reaction (4)) can lead to sterically hindered radical sites which cannot add to acrylate double bonds.¹⁵ The conversion of these radicals to thiyl species through hydrogen abstraction can be viewed as a restoration of their propagating ability.

The thiyl radicals formed during cure are resistant to both recombination and reaction with oxygen,^{16,17} as compared to their carbon analogues. Thus we can expect a higher concentration of thiyl radicals in the late stages of cure than is possible with carbon radicals ($R\cdot$). Development of favorable mechanical properties is strongly linked to the extent of crosslinking, which occurs during this period. Hence the replacement of $R\cdot$ by $Y-S\cdot$ will result in a more efficient use of the radical “potential” built up during initiation, and therefore a more thoroughly cured film.

Propagation of cure by thiyl radicals results in the formation of a large number of thioether ($R^1CH_2-S-CH_2R^2$) linkages in the crosslinked network. This is a flexible bond¹⁸ that can increase the strain tolerated by the polymer film without breakage. Even more added structural stability can result if multifunctional thiols are used. In this case, thiol molecules can lead to additional crosslinks in the acrylate network once their functional ends connect initially separated chains.

3.1 Results

We investigated the effects of formulating UV and EB curable coating solutions with small amounts of the tetrathiol, PETMP. A series of UV coating formulae with 0.0, 15.3, 20.5, and 45.8 mmol/kg PETMP was prepared, coated on Leneta, and cured with UV exposure varying between 146 and 882 mJ/cm². MEK double rubs were performed, and the results of these evaluations are shown in Figure 2.

In Figure 2, (a) is the cure response of a control EOTMPTA coating with no added thiol. It conforms to the typical sigmoid shape, with a lower “rubbery” and upper “glassy” plateau, which bound the central domain where rapid development of mechanical properties occurs. The plots (b) and (c) show a peak in MEKR values, which begins after 500 mJ/cm² UV exposure. Note that the points following the peak exposure domain belong to the unmodified glassy plateau region as detected in (a).

Increasing the concentration of PETMP from 15.3 mmol/kg in (b) to 20.5 mmol/kg in (c) results in an increase in the height of this peak, from 42 to 51 MEKR. Furthermore, the length of the peak region (range of UV exposure values corresponding to large MEKR) increases—in the direction of higher irradiation—with greater concentrations of PETMP. While 600 mJ/cm² gives only 30 MEKR in (b), this exposure corresponds to the maximum MEKR value of 51 in (c).

Finally, as shown in (d), a concentration of 45.8 mmol/kg PETMP results in a cure response curve that has returned to the sigmoid shape of (a). However, while the lower plateau region is at similar MEKR values between the two, the control curve (a) provides 33 MEKR at the upper plateau and curve (d) has an upper plateau at 50 MEKR. Thus hugely improved mechanical properties are obtained at the glassy plateau with a sufficient formulated level of PETMP.

An analogous experiment was conducted with EB curing. We prepared a series of EB coating formulae containing 0.0, 2.0, 4.1, and 6.1 mmol/kg PETMP. These were applied to Leneta cards and cured with EB dose varying from 10 kGy to 35 kGy. MEKR results for these cured films are presented in Figure 3.

These EB cure response curves mirror the ones obtained for the UV cured system: the character of the curve, and the MEKR values obtained, depends on the amount of PETMP added. Figure 3, (a) is a control sample with no PETMP. The glassy plateau begins at a dose of about 25 kGy, and

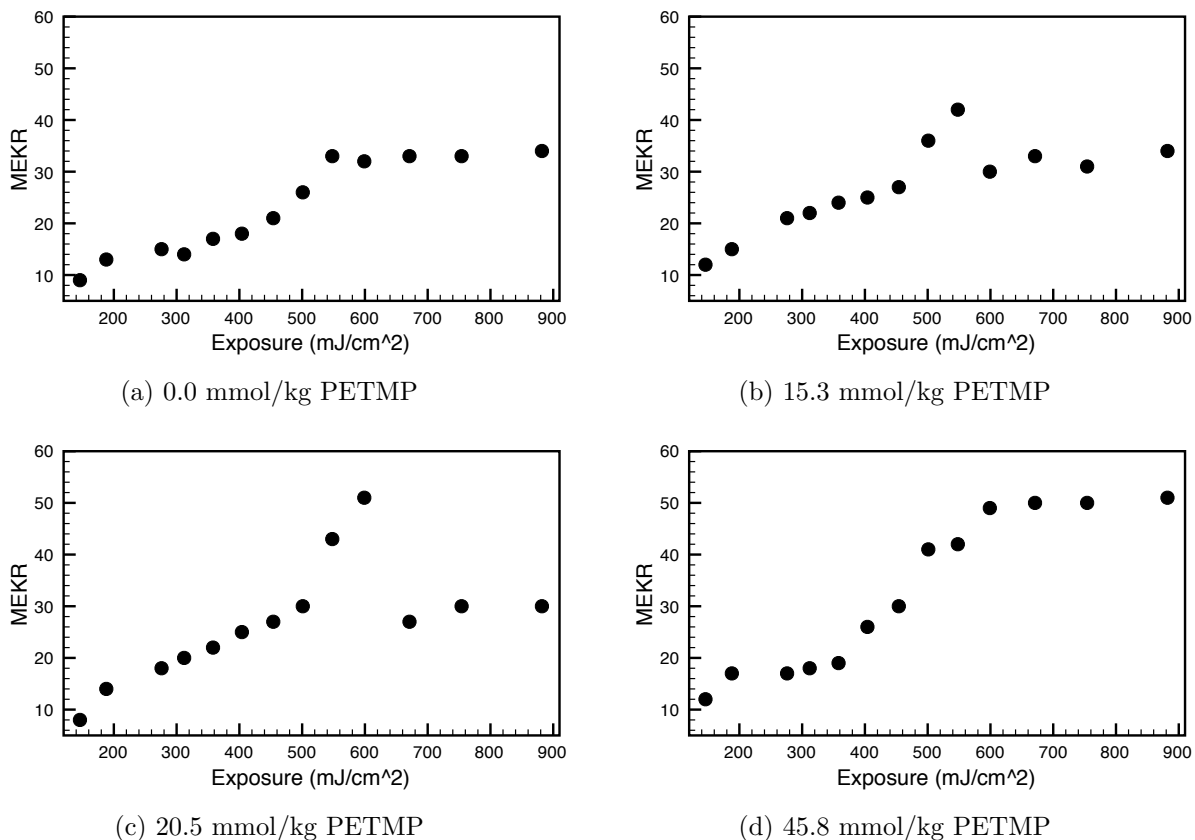


Figure 2: UV cured EOTMPTA on Leneta, US # 3 rod, with varying concentration of PETMP in plots (a–d). A peak in MEKR appears in the upper (glassy) plateau region at intermediate PETMP concentrations. The peak disappears once a sufficient amount of the tetrathiol is added. The final glassy plateau in (d) is at significantly greater MEKR numbers than the one in (a).

11 MEKR are obtained in this final regime. In the cure response plots (b) and (c), there are peaked upper plateau regions. The doses for this peak range from 22–28 kGy and 22–33 kGy, respectively, and about 15 MEKR are obtained. Once 6.1 mmol/kg PETMP is added, as in plot (d), the sigmoid shape is restored. Additionally, a much greater glassy plateau MEKR value, over 20 (double that of the control), is obtained for these cure conditions.

3.2 Colloidal Model for Acrylate Polymer Growth

To explain the shape of the cure response curves for UV and EB coating solutions, as the concentration of PETMP is varied, we introduce a qualitative, two-stage colloidal model for polymer growth during radiation cure. In the first stage of curing, radicals are formed through initiation processes and begin to propagate by adding to the plentiful monomer double bonds. These growing chains are distributed stochastically throughout the liquid monomer solution. Chain addition propagates outward from these sites, radiating into the free surrounding monomer. Once most of the eventual double bond conversion is complete, the film will contain tightly crosslinked, highly branched do-

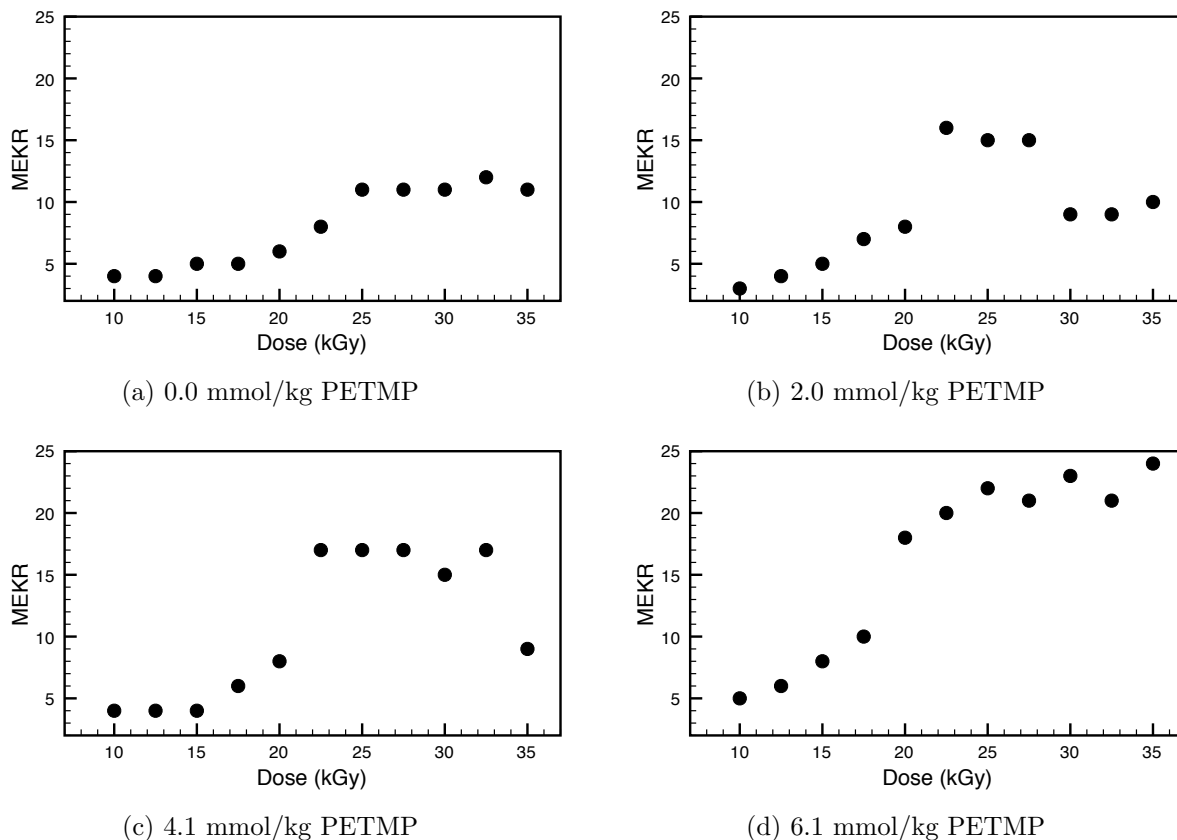


Figure 3: EB cured EOTMPTA on Leneta, US # 3 rod, 200 ppm O₂. Concentration of PETMP is varied in plots (a–d). Cure responses evolve from the standard sigmoid shape in (a), through curves with peaked domains in (b) and (c), and back to an “amplified” sigmoid character in (d).

mains (corresponding to the beginning sites of initiation) separated by a more weakly-connected polymer with fewer crosslinks.

While there are domains of dense, nearly infinite molecular weight polymer of high modulus, these are connected by a much lower modulus material. The low MEKR obtained at the early, rubbery plateau in a cure response curve corresponds to the material failing at the weak regions connecting the colloidal, spherical domains of high crosslink density. The transition between rubbery plateau, at low MEKR, to glassy plateau, at high MEKR, corresponds to the fusion of colloidal domains into a more rigid global network.¹⁹ We find that the propagation chemistry occurring during this transition is key to determining the polymer strength.

As evidenced by the sustained high MEKR values at the glassy plateau in Figures 2, (d) and 3, (d), crosslinked polymer produced in the presence of multifunctional thiols is stronger than that produced without a thiol. Due to the extremely high chain transfer constant of thiols, it is reasonable to assume that carbon radicals are converted to thiyl radicals as rapidly as they form. Therefore, the early stages of cure—building of colloidal domains of active propagation—always involve thiyl addition to C=C bonds. However, with greater applied doses of radiation, the number of initiating radicals increases. The final stage of cure, vitrification through the fusion of colloidal domains, will

Table 1: Crossover exposure values for UV-cured EOTMPTA coatings with PETMP. The crossover is obtained by linear interpolation in the abscissa of the cure response curve, between the final peaked point and the first non-peaked plateau point.

[PETMP] (mmol/kg)	[SH] (mmol/kg)	Exposure (mJ/cm ²)
15.3	61.2	574
20.5	82.0	635
45.8	183.2	> 882

Table 2: Crossover dose values for EB-cured EOTMPTA coatings with PETMP. Crossover is defined and calculated in the same manner as for UV results in Table 1.

[PETMP] (mmol/kg)	[SH] (mmol/kg)	Dose (kGy)
2.0	8.0	28.8
4.1	16.4	33.8
6.1	24.4	> 35.0

take place predominantly by the propagation mechanism corresponding to the radical species of greatest concentration.

If the number of available thiol groups exceeds the number of initiating radicals, the final stages of cure will also be dominated by the thioether-forming addition of $Y-S\cdot$ to $CH_2=CHX$. However, if the concentration of $R\cdot$ (carbon centered radical) is greater than $Y-S\cdot$ at the end of cure, the more rigidly crosslinked all-acrylate polymer will be the material which solidifies the overall network. MEKR results show this brittle linking material to be much less rub resistant than the flexible thioether-containing polymer produced through thiyl addition.

3.3 Thiol Groups Titrate Radicals

Based on the colloidal model of acrylate photopolymerization, we have inferred a quantitative link between the total concentration of thiol groups, [SH], and the exposure at which the rate of carbon radical propagation exceeds the rate of thiyl radical propagation. For convenience, we refer to this as the crossover point for the given SH concentration. Equivalently, for each level of radiation exposure within the glassy plateau, we can associate a number [SH] of thiol groups such that the given exposure is the crossover point between peak and low plateau MEKR values. This concentration of thiol groups is not expected to equal the total number of radicals formed at initiation. Rather, it is the number of propagating radicals contributing to the development of mechanical properties, and available for chain transfer to yield thiyl radicals.

The crossover points for the UV-cured data series (Figure 2) were calculated by taking the midpoint exposure between the end of the peak region and the start of the low glassy plateau region. These crossover exposure values are given in Table 1. We could only determine a lower bound for the crossover point with [SH] = 183.2 mmol/kg, as the (thiyl addition) peak domain extends throughout all the glassy plateau points—that is, no crossover is observed. Analogous

calculations were performed for the EB-cured series in Figure 3 and can be found in Table 2. Again, only a lower bound for the crossover dose with 24.4 mmol/kg thiol groups could be found in EB. By varying [SH] and determining the crossover point in this way, we titrate the number of radicals formed at each measured crossover exposure. A plot of MEKR at a fixed exposure against [SH] will have the form of a titration curve.

By linear interpolation of the crossover data, we found that a 600 mJ/cm² UV exposure required a thiol group concentration of 70 mmol/kg for equivalence with propagating radicals. For an EB dose of 30 kGy, the necessary value of [SH] was 10 mmol/kg. Hence we have measured the ratio of propagating radicals in UV curing to that in EB as 7 : 1.

The fact that far fewer radicals are produced in EB cure, as compared to UV, is not surprising as there are clearly pronounced differences in the mechanical properties of UV and EB cured coatings. The UV control cure response in Figure 2, (a) has a glassy plateau with over 30 MEKR, while the EB control curve, Figure 3, (a), shows only 12 MEKR at this plateau.

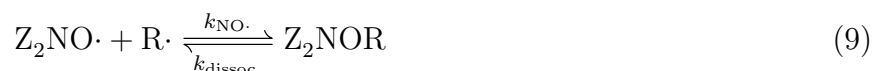
Formulated concentration of photoinitiator in our UV cured samples was 2.0 % (w/w) Irgacure 2959, or [PI] = 89.17 mmol/kg. The published quantum yield for dissociation, Φ , of Irgacure photoinitiators ranges from 0.2 to 0.6.²⁰⁻²² Thus, using $\Phi = 0.6$, the maximum concentration of radical pairs produced is

$$\Phi \cdot [\text{PI}] = 53.5 \text{ mmol/kg.} \quad (8)$$

Doubling this value, since there are two free radicals originating from each radical pair, we find the predicted maximum concentration of initiating radicals to be 107 mmol/kg. Comparison to the 70 mmol/kg concentration of propagating radicals, as measured by titration with thiol groups, shows that fewer radicals than the theoretical maximum actually contribute to cure.

4 Radical Complexation and Cure Efficiency

The use of nitroxides as inhibitors for in-can storage stability of polymerizable materials²³ and in nitroxide mediated polymerization (NMP)^{24,25} is well-known. Stable nitroxide radicals react with propagating radicals to form weakly bonded NOR complexes. The equilibrium



is established,²⁶ where $\text{Z}_2\text{NO}\cdot$ is the hindered nitroxide radical (Z represents one of the two organic groups bonded to the central nitrogen), $\text{R}\cdot$ is a propagating radical, and Z_2NOR is the complex, also known as an alkoxyamine. The forward ($k_{\text{NO}\cdot}$) and backward ($k_{\text{dissoc.}}$) rate constants of complexation are defined by reaction (9).

When complexed, $\text{R}\cdot$ is protected from recombination and reaction with oxygen. As discussed earlier, it is these two termination processes that reduce most prominently the rate of cure and hence development of a strong polymer network.

Inclusion of a small number of nitroxides in the radiation curable formula can add selectivity to the polymerization process, favoring addition over termination. At optimum curing conditions, i.e. nitroxide concentrations, we expect an increase in cure efficiency: equal or improved mechanical properties with lower input of energy. However, nitroxide materials are radical scavengers. Large concentrations of such inhibitors will retard the development of mechanical properties to greater dose—more initiating radicals need to be produced to overcome the inhibition effect.

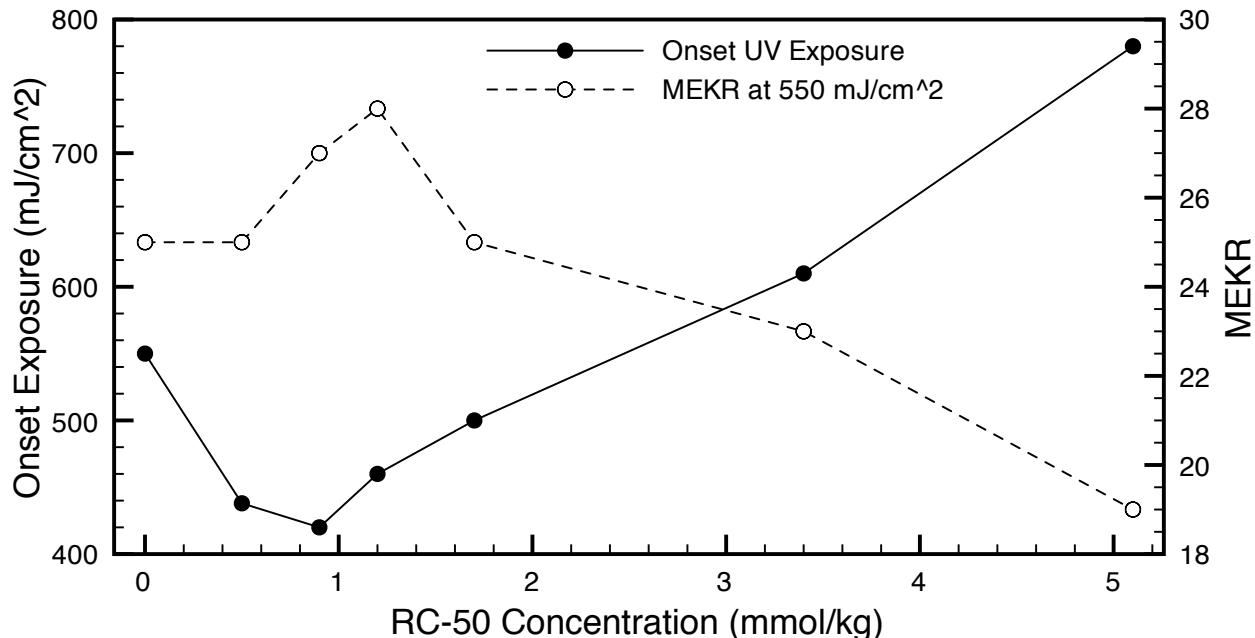


Figure 4: UV cured EOTMPA with varying BlocBuilder RC-50 concentration. Exposure for onset and glassy plateau MEKR (at 550 mJ/cm²) are shown.

4.1 Onset Point Characterization

In this section, we address the efficiency of photopolymerization of an acrylate formula. For this analysis, we define a quantitative means of characterizing cure efficiency, called the onset point, with corresponding onset dose (in EB) or exposure (in UV).

Typical cure response curves, or plots of MEKR versus irradiation intensity, for EOTMPTA by UV and EB were shown as Figures 2, (a) and 3, (a), respectively. The values of MEKR obtained in such plots depend on a variety of factors—coating thickness, humidity, random variations in rubbing pressure, and of course, the individual carrying out the measurement. However, the general trend of the curve with increasing dose or exposure, from a low MEKR rubbery plateau, to a region of rapidly increasing MEKR, and finally to the glassy plateau with high MEKR, depends only on the dynamics of cure.

We define cure efficiency in terms of the exposure at which the greatest rate of change in MEKR with exposure is attained, i.e., the inflection point of the cure response curve. Mathematically, this is the point at which the second derivative of MEKR versus exposure equals zero. This point is referred to as the onset point, and we will refer to onset exposure or onset dose in the respective UV and EB cases. The onset point is a useful characterization of the cure dynamics—more efficient polymerization will decrease the exposure required for onset, while inhibition of cure will increase it.

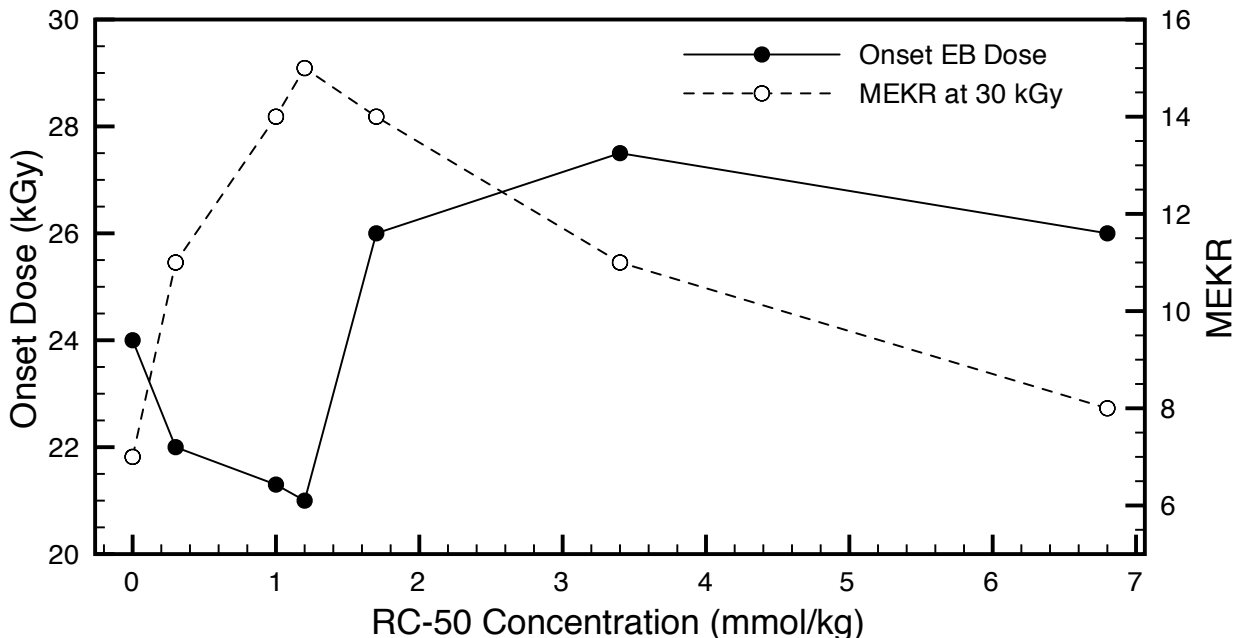


Figure 5: EB cured EOTMPTA with varying concentration of BlocBuilder RC-50. Dose for onset and glassy plateau MEKR (at 30 kGy) are shown.

4.2 Results

We prepared a series of coating solutions for UV and EB curing containing the three nitroxides UV 10, RC-50, and DBuN (Figure 1). UV 10 was varied between 0 and 3.3 mmol/kg in UV and up to 3.4 mmol/kg in EB solutions. RC-50 was included up to 5.1 mmol/kg in UV samples, and to 6.8 mmol/kg in EB cured formulae. Finally DBuN was used between 0 and 6.5 mmol/kg in UV curing, and up to 12.5 mmol/kg in EB curing.

To illustrate the effect of nitroxides on onset alongside MEKR, the onset point (in mJ/cm^2) and the MEKR obtained at an exposure of $550 \text{ mJ}/\text{cm}^2$, near the glassy plateau, were compared for RC-50 in UV-cured EOTMPTA. These UV results are given in Figure 4. The same experiment was conducted with RC-50 in EB-cured formulae. We determined the EB dose for onset (in kGy) and recorded the glassy plateau MEKR at 30 kGy; the results are plotted in Figure 5.

In both UV and EB curing, we see the same general trend as RC-50 concentration is increased. First a decrease in onset exposure, which is accompanied by an increase in glassy plateau MEKR. After a minimum onset (maximum MEKR) is achieved, the inhibitory effects of the nitroxide become clear as the concentration of stable radicals increases. Onset and MEKR rise and fall, respectively, bounding the useful range of RC-50 concentration in radiation curable formulae. In general, decreases in onset dose result in increases in the MEKR at the glassy plateau—it is therefore sufficient to consider only the onset effect of nitroxides in evaluating their performance.

The onset effects of UV 10, RC-50, and DBuN were compared in both UV and EB cured EOTMPTA coatings. UV onset point data is shown in Figure 6 and the corresponding EB data is in Figure 7. In each case, there is a nitroxide concentration such that the onset point is minimized

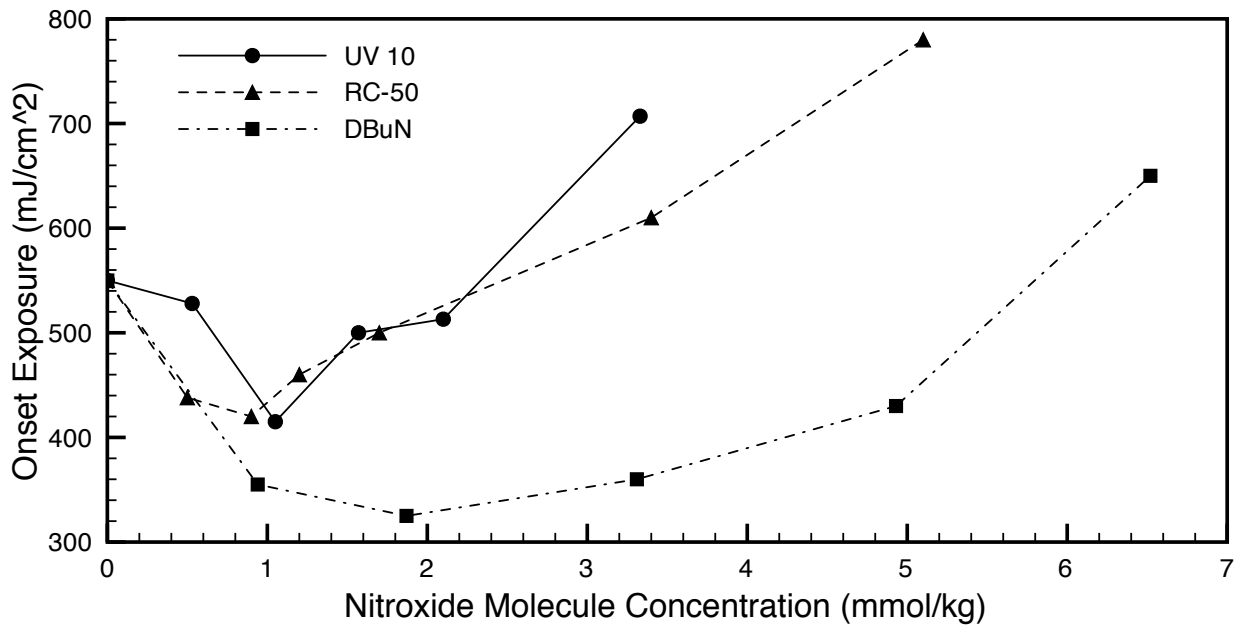


Figure 6: UV onset exposure values for the nitroxides UV 10, RC-50, and DBuN at varying concentration in EOTMPTA.

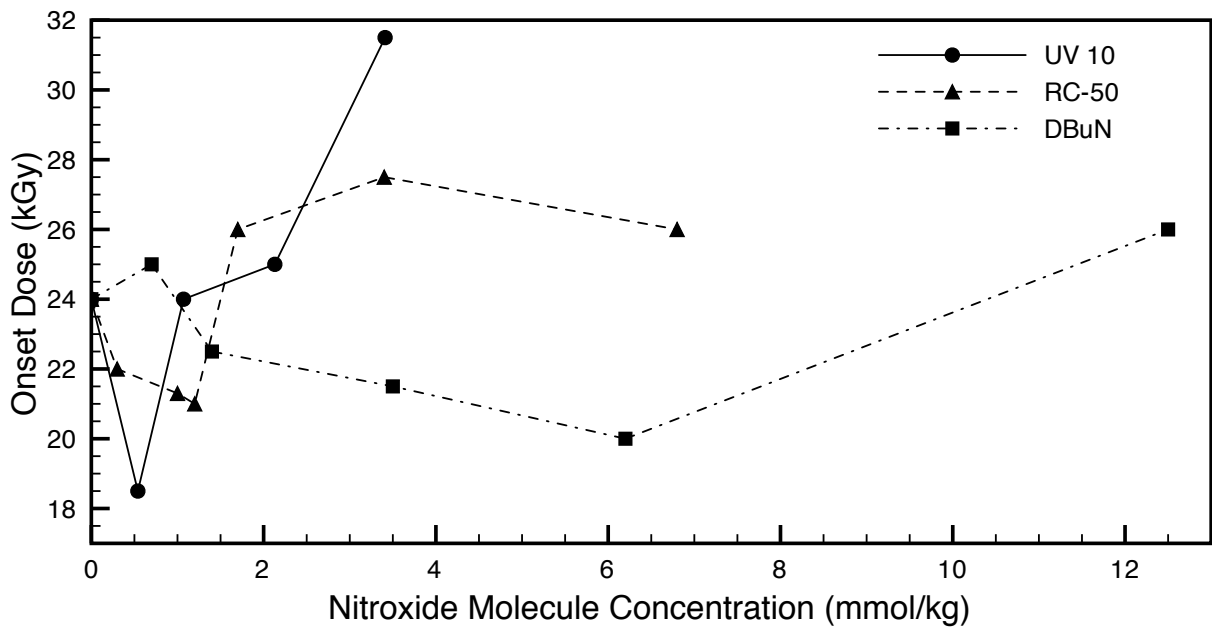


Figure 7: EB onset dose values for the nitroxides UV 10, RC-50, and DBuN at varying concentration in EOTMPTA.

(and certainly, decreased relative to control). All three nitroxides show the characteristic inhibition effect of increasing onset at high concentrations.

In UV and EB cure, UV 10 causes an early (i.e., with low concentrations) drop in onset, followed quickly by an increase in onset, giving it a small window for improving efficiency. RC-50 gives onset improvement starting from roughly the same concentrations as UV 10; RC-50 onset minimum is at a slightly smaller concentration in UV and a slightly higher one in EB. However, the inhibition behavior of RC-50 at higher concentrations has an onset increase with slope lower than that for UV 10. RC-50 therefore has a somewhat larger formulation window. In contrast to the other two nitroxides, DBuN requires much greater concentrations for both optimization of onset and for the beginning of its inhibitory effects. This nitroxide has a very wide window for formulation without inhibition of cure.

4.3 Discussion

As observed in Figures 4–7, formulation of nitroxide species in radiation cure coating solutions leads to increased cure efficiency, and therefore better mechanical strength, when the concentration of nitroxides is chosen carefully. We can analyze these results in terms of the colloidal cure model.

The onset point is the critical exposure between rubbery plateau and glassy plateau cure response. At the onset, enough radicals are produced so that by the end of cure, fusion of colloidal domains has begun. Shifting of onset to lower values indicates that the smaller number of radicals initially produced at this onset exposure is sufficient to begin vitrification of the polymer network.

In analogy to NMP,²⁴ propagating radicals are stored in the form of alkoxyamines during initiation and in the early stages of propagation, as in equation (9). In this non-radical alkoxyamine form, the carbon radical is much less reactive toward oxygen and other carbon radicals. Radical-radical recombination and oxygen inhibition depend on the interaction of two radical species.

While the complexation reaction decreases the number of propagating radicals, the nitroxide concentrations we consider here are generally much lower than the concentrations of propagating radicals as measured by thiol titration. Radical concentration is greatest during the early stages of cure, and in this timespan the decrease in radical concentration due to complexation is insignificant when optimum (non-inhibiting, see Figures 6 and 7) nitroxide levels are used. Figure 7 clearly shows that inhibition always results from nitroxide concentrations approaching the initiating radical concentration. Depending on the nitroxide in question, concentrations of stable radicals much lower than the initiating radical concentration can still cause inhibition (UV results in Figure 6 illustrate this).

As cure progresses to the state of colloidal, highly-branched domains suspended in less densely packed polymer, far fewer radicals are available for propagation due to inevitable termination reactions. The alkoxyamines formed from nitroxides and carbon radicals in earlier stages of cure now become pivotal. Dissociation of the alkoxyamine complex is slow relative to the formation of alkoxyamines, but its decay to nitroxides and carbon radicals on the timescale of late cure (vitrification) dynamics makes the alkoxyamine a time-delayed radical source. The released carbon radicals contribute to the fusion of colloidal domains to further the vitrification of the cured polymer network. By this delayed use of radicals when their concentration is most valuable, better mechanical properties can be realized with a lower input of radiation energy. The decrease in onset exposure coupled with an increase in MEKR at certain nitroxide concentrations (Figures 4–7) is the measurable result of the change in radical reactivity afforded by complexation.

The concentration position of an onset minimum and the width of the non-inhibiting window depends intimately on the nitroxide structure as it affects the energetics of the NO–R bond. Materials which rapidly complex propagating radicals, that is, have a high k_{NO} , will tend to shorten the concentration window if k_{dissoc} is small. In this case the nitroxide acts as a strong radical trap inhibitor, forming many alkoxyamines which dissociate very slowly. UV 10 is consistent with these rates, as it has an early onset minimum (high k_{NO}), with inhibition beginning upon increasing concentration by a small amount (low k_{dissoc}). Greater concentrations of RC-50 are required for its inhibition effects to show. The alkoxyamines formed with RC-50 likely dissociate more rapidly, that is, with somewhat higher k_{dissoc} . In the low k_{dissoc} limit, all concentrations of nitroxide would be inhibiting.

Compared to UV 10 and RC-50, DBuN requires a higher concentration for onset improvement, and even greater concentrations for inhibition to begin. This nitroxide’s cure behavior is consistent with high k_{dissoc} and relatively low k_{NO} . Too great a k_{dissoc} value without a reasonably high k_{NO} constant will result in radicals and nitroxides being released early in cure, diminishing the onset improvement that depends on radical concentration in late cure. If the alkoxyamine complex is too transient, it cannot benefit cure efficiency.

5 Radical Storage and Latent Cure

The complexation of propagating radicals with nitroxides results in stored radicals that persist after the main radiation cure event. The direct product of radical complexation, an alkoxyamine, is known to decompose thermally.^{27–30} Other long-lived but thermally unstable species may be formed by reaction of the nitroxide with peroxy radicals (resulting from oxygen inhibition).^{27,31–34} Photo-generated radicals are channeled into stored radical potential.

Thus we can view radiation curing as a process which “arms” the system for a second, thermally initiated cure event. Post heating the cured film can re-activate stored radicals and lead to further development of mechanical properties.

As mentioned previously, the initial charge of nitroxide radicals causes alkoxyamines to be formed in situ as radiation curing occurs. A second method of introducing alkoxyamines to the photocured film is to add them directly to the coating solution. We investigated both sources of stored radical potential for latent cure effects.

5.1 Latent Cure Kinetics

We examined the change in MEKR of a cured film as a function of time spent at elevated temperature. Radiation cured films on Leneta were placed in an oven for a length of time t (in minutes), and upon removal and equilibration to room temperature, MEKR were recorded; this value is denoted $\text{MEKR}(t)$. One Leneta card was used for each time point: MEKR evaluation was conducted on a newly removed coated film at each t . We define the change in MEKR after a heating time t , $R(t)$, by

$$R(t) = \text{MEKR}(t) - \text{MEKR}(t = 0), \quad (10)$$

where $\text{MEKR}(t = 0)$ is the result obtained without heating the sample. The infinite-time limit of $R(t)$ is denoted by

$$R_{\infty} = \lim_{t \rightarrow \infty} R(t). \quad (11)$$

Table 3: Empirical fit of $R(t)$ versus time for the nitroxides UV 10, RC-50, and DBuN. See text for explanation of the fit parameters R_∞ and k .

Nitroxide	T ($^{\circ}\text{C}$)	R_∞ (MEKR)	k (10^{-4} s^{-1})
UV 10 (2.1 mmol/kg, EB)	80	4.8	5.47
	100	5.2	16.10
RC-50 (2.1 mmol/kg, UV)	80	14.2	10.18
	115	12.9	25.47
DBuN (12.5 mmol/kg, UV)	60	17.0	2.05
	80	18.7	2.72

A large value for R_∞ means that a high degree of post curing can occur, while the rate of change of $R(t)$ establishes the kinetics of latent cure development.

We fit the $R(t)$ versus t data to the empirical, two-parameter equation

$$R(t) = R_\infty \exp\left(-\frac{1}{kt}\right), \quad (12)$$

where k is the rate parameter for the data set, and the limiting R_∞ value is an adjustable parameter as well. The best fit parameters were determined using a plot of $\ln R(t)$ versus $\frac{1}{t}$. Linear regression analysis on the data in this form provided the intercept, $\ln R_\infty$, and slope, $-\frac{1}{k}$, of the line:

$$\ln R(t) = \ln R_\infty - \frac{1}{kt}. \quad (13)$$

We do not assume any particular reaction order holds for the development of $R(t)$; the given model simply provides a convenient fit to the data. The actual mechanism governing the evolution of $R(t)$ is likely a complex series of reactions.

5.2 Results

The nitroxide UV 10, at a concentration of 2.13 mmol/kg, was examined for latent cure after EB curing at 30 kGy. $R(t)$ was recorded versus time at temperatures 80 $^{\circ}\text{C}$ and 100 $^{\circ}\text{C}$. RC-50 was used in UV curable EOTMPTA at 2.1 mmol/kg, with exposure 541 mJ/cm². The temperatures of study were 80 $^{\circ}\text{C}$ and 115 $^{\circ}\text{C}$. Finally DBuN was examined at 12.5 mmol/kg in UV curable EOTMPTA with 554 mJ/cm² exposure, at the temperatures 60 $^{\circ}\text{C}$ and 80 $^{\circ}\text{C}$.

Samples were heated for durations t between 10 and 300 minutes at the given temperatures. MEKR values were recorded, and from these we calculated $R(t)$. The results of the empirical fit procedure, discussed above, are given in Table 3. Rate parameters k were obtained directly in units of min⁻¹, and were converted to reciprocal seconds for display here.

The temperature dependence of rate parameters k in Table 3 was fit to the Arrhenius equation.³⁵ For each nitroxide, we obtained Arrhenius activation energies and pre-exponential factors, which are given in Table 4. The activation energies follow the order: UV 10 > RC-50 > DBuN.

Table 4: Arrhenius activation energy E_a and pre-exponential factor A for latent cure development in time with the nitroxides UV 10, RC-50, and DBuN.

Nitroxide	E_a (kJ/mol)	A (s^{-1})
UV 10	59.2	3.12×10^5
RC-50	29.8	2.62×10^1
DBuN	13.8	2.99×10^{-2}

Table 5: Change in MEKR after 100 minutes at elevated temperature: $R(100 \text{ min})$. 3.5 mmol/kg UV 10, 7 mmol/kg RC-50 and DBuN. UV cure at 550 mJ/cm².

Nitroxide	60 °C	80 °C	100 °C
UV 10	5	15	20
RC-50	12	16	23
DBuN	4	7	8

We compared the latent cure properties of UV 10, RC-50, and DBuN under similar conditions: 7 mmol/kg total concentration of nitroxide groups (3.5 mmol/kg of the difunctional UV 10), UV cure at 550 mJ/cm², followed by 100 minutes heating at temperatures 60 °C, 80 °C, and 100 °C. At these concentrations, the nitroxides were within their inhibiting ranges. Therefore the number of alkoxyamine complexes formed was expected to be high. The results, MEKR increase after heating, are given in Table 5.

While UV 10 and RC-50 afford a similar MEKR increase at 80 °C and 100 °C, RC-50 is able to provide relatively large MEKR gains at 60 °C. DBuN, at the concentration used (lower than in Table 3), gives relatively low MEKR increases even when heated for long times at 100 °C.

To demonstrate that alkoxyamines (NOR compounds) are a source of stored radicals that can be activated upon heating, we prepared EOTMPTA coating solutions containing Tinuvin 123 at the concentrations 0, 3.8, 11.8, and 23.4 mmol/kg. These were cured by UV with an exposure of 550 mJ/cm², and subjected to heating for 100 minutes at the temperatures 60 °C, 80 °C, and 100 °C. The change in MEKR, or $R(t)$ with $t = 100 \text{ min}$, is plotted as a function of Tinuvin 123 concentration and temperature in Figure 8.

Rapid change in $R(100 \text{ min})$ with increasing Tinuvin 123 concentration was observed only between 0 and 3.8 mmol/kg. It is interesting to note the modest decrease in R from Tinuvin 123 at 3.8 mmol/kg for greater concentrations of the alkoxyamine at 60 °C and 80 °C.

The thermal post-cure with Tinuvin 123 was evaluated with coatings cured by EB at both normal and elevated oxygen concentrations. Results are given in Table 6, for 200 and 700 ppm O₂, after 140 minutes at elevated temperature, with either 0 or 23.4 mmol/kg alkoxyamine. The effect of Tinuvin 123 on post cure, compared to a sample without alkoxyamine, is large at 700 ppm O₂. Barely any latent cure is observed without alkoxyamine at this oxygen concentration. Lowering the O₂ to 200 ppm allows much more significant post cure with no alkoxyamine.

Finally, we examined both onset and latent cure effects for a sample containing DBuN and

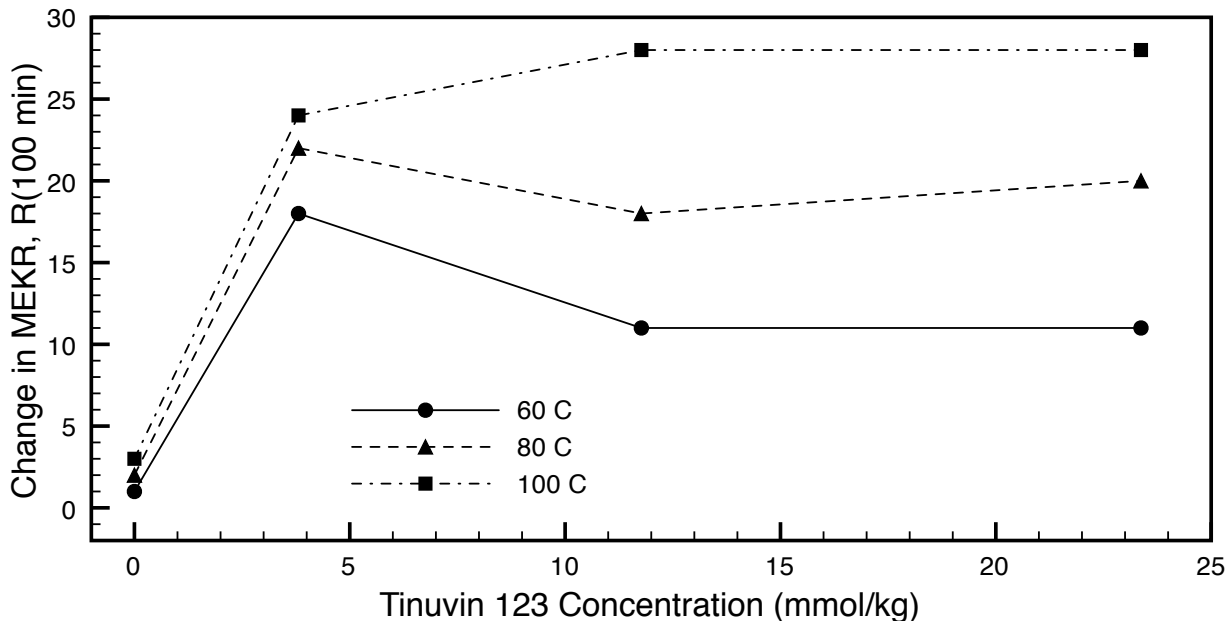


Figure 8: Change in MEKR following heating of UV EOTMPTA coatings containing the alkoxyamine Tinuvin 123. UV cure at 550 mJ/cm^2 exposure, followed by 100 minutes at $60 \text{ }^\circ\text{C}$, $80 \text{ }^\circ\text{C}$, or $100 \text{ }^\circ\text{C}$.

Tinuvin 123 at their optimal levels (Figures 6 and 8). A UV curable coating solution with 2.2 mmol/kg DBuN and 4.6 mmol/kg Tinuvin 123 was prepared. The UV onset exposure obtained was 336 mJ/cm^2 ; this is comparable to the onset point realized with 2 mmol/kg DBuN alone. The MEKR increase with 100 minutes heating at $100 \text{ }^\circ\text{C}$ was 12, compared to an increase of 3 for the base EOTMPTA coating with UV cure. The significant improvement relative to control establishes that onset (cure efficiency) enhancement and increased latent cure potential can be realized simultaneously.

Table 6: MEKR increase with variable O_2 levels in EB. Coatings cured at 30 kGy and heated 140 min at the specified temperature. Oxygen concentration is the approximate instrument readout at time of irradiation.

O_2 (ppm)	Tinuvin 123 (mmol/kg)	$60 \text{ }^\circ\text{C}$	$80 \text{ }^\circ\text{C}$	$100 \text{ }^\circ\text{C}$
200	0.0	1	5	11
200	23.4	3	8	15
700	0.0			5
700	23.4			16

5.3 Discussion

We notice both the rate and extent of development of mechanical strength in a post-heating process depends closely on the identity of the nitroxide originally present in the coating solution. Table 4 shows that UV 10, RC-50, and DBuN show significantly different activation energies for thermal re-initiation of cure. Thermal initiation with UV 10 takes the highest energy, with RC-50 requiring less, and DBuN needing the least.

According to the onset results in Figures 6 and 7, the rate constant of alkoxyamine dissociation, $k_{\text{dissoc.}}$ seemed to scale as UV 10 < RC-50 < DBuN, while k_{NO} appeared to scale in the opposite direction. That is, UV 10 complexes tended to form rapidly and dissociate slowly, while at the other extreme, DBuN complexes form more slowly and dissociate rapidly. Measurements of $k_{\text{dissoc.}}$ for TEMPO (of which UV10 is a derivative), RC-50, and DBuN agree with our ordering.²⁹

The ordering of activation energies (Table 4) for thermal post-cure, UV 10 > RC-50 > DBuN, agrees with our onset measurements as well. Namely, nitroxide species which lead to more thermally stable (but still accessible) stored radicals also inhibit cure (raise onset) starting from a lower concentration, forcing the optimal concentration for onset lowering to be less.

Activation energies for thermal post-cure measured here are nearly an order of magnitude lower than published activation energies for dissociation of TEMPO, RC-50, and DBuN alkoxyamines with a number of alkyl groups.^{29,30} Therefore, the rate determining step for latent cure is almost certainly not dissociation of an alkoxyamine, which would be the simplest mechanism for thermal initiation. The generation of highly oxidized species based on the nitroxide has been suggested within the mechanism of polymer stabilization by hindered amine light stabilizers (HALS).²⁷ The source of stored radical potential, judging by the activation energies in Table 4, is much easier to fragment than an alkoxyamine, which would require far higher temperatures for significant thermal initiation.

According to Table 5, RC-50 and UV 10 store significantly more radicals than DBuN. Since the rate of DBuN alkoxyamine dissociation, $k_{\text{dissoc.}}$ is much greater than for the other nitroxides, this is the expected result. Fewer alkoxyamines survive past the early stages of cure, so there is much less radical storage by this nitroxide. More latent cure can be achieved at lower temperatures with RC-50 than with UV 10. The measured activation energies for thermal initiation (in EB for UV 10 and UV for RC-50, Table 4) are consistent with this ordering.

Latent cure following UV irradiation has proven much more effective (that is, granting much higher MEKR improvements) than after EB cure. Compare $R_{\infty} = 5$ for EB-cured UV 10 containing solutions, heated at 100 °C (Table 3) to the 20 MEKR increase with 100 minutes at 100 °C for UV-cured UV 10 solutions (Table 5). Since fewer radicals are formed during EB initiation, storage of any significant number of radicals for latent cure would be highly detrimental to the EB cure itself.

As seen in Figure 8, the addition of alkoxyamines to radiation curable coating solutions does lead to thermal cure potential. However, the effect does not simply scale with alkoxyamine concentration: after a limit of about 5 mmol/kg Tinuvin 123 (in UV curable solutions), little improvement in post cure with additional alkoxyamine is observed. There are more factors limiting stored radical potential than nitroxide and propagating radical concentrations—the parameters which govern alkoxyamine formation. We postulated that highly oxidized species may be the actual carriers of stored radicals, so the concentration of oxygen (and hence concentration of peroxy radicals, ROO·) in the acrylate film during cure may be critical in determining the extent of radical storage.

We were able to investigate post cure effects at varying oxygen concentrations with EB curing, by using a less effective inerting procedure. A very high Tinuvin 123 concentration was compared to EB curable EOTMPA samples without alkoxyamine in Table 6. When cured at a typical O₂ level for good inerting, 200 ppm, Tinuvin 123 showed a modest latent cure effect compared to plain EOTMPA. Increasing the O₂ concentration at cure to 700 ppm resulted in very poor MEKR improvement for the alkoxyamine-free sample, but even better post-cure for the sample with Tinuvin 123 than was seen at 200 ppm oxygen. Evidence is thus provided for the claim that oxygen (and most likely peroxy radicals) are key intermediates in the storage of radicals for latent cure.

Given the small onset improvement window observed for UV 10 and RC-50 (Figures 6, 7), it is obvious that the conditions which favor storage of radicals, through an initial alkoxyamine and ending in a more oxidized species, do not allow the improvement of photocure dynamics as measured by onset lowering. However, once alkoxyamines are present in the system (such as their introduction at the point of formulation, as with Tinuvin 123), stored radical potential develops with little regard to photocure dynamics. Hence, the use of low concentrations of nitroxide to lower onset while simultaneously generating stored radicals with an alkoxyamine (added at formulation) and peroxy radicals (or other oxygenated species) has proven quite reasonable.

6 Conclusions

The photoinitiated free radical polymerization of acrylates in modern applications requires extremely rapid conversion using high concentrations of initiating radicals. The molecular architecture of the polymer generated is thus largely uncontrolled. We have explored several distinct means of altering photopolymerization dynamics, and hence final mechanical properties, through the intelligent control of free radical reactivity.

Partial replacement of carbon centered radicals with sulfur centered thiyl radicals (from chain transfer to a thiol) results in a propagating species that is resistant to radical-radical recombination and oxygen inhibition. Furthermore, the thioether bonds produced in the cured film add strength and flexibility.

Competition between this thiyl addition and standard acrylate propagation provided an interesting means of probing the growth of cured domains through space, and led to the development of a colloidal model for acrylate polymerization. Based on this model and the data showing competition between thiyl and acrylate addition, we were able to estimate that seven times more radicals are produced in UV cure than in the EB process.

Within a narrow range of concentrations, stable nitroxide radicals afford benefits in cure efficiency, as measured by a lowering of the onset point, or dose required for the beginning of vitrification, along with an increase in the eventual MEKR obtained. The reversible complexation of radicals (in the form of alkoxyamines) grants them an effectively longer lifetime: radicals that would be terminated in the early stages of cure are complexed rapidly, and these complexes dissociate during late cure, when the total radical concentration has been greatly reduced and a small increase in radical concentration leads to a much greater extent of vitrification.

It was found that the presence of alkoxyamines during photocure (generated in situ from nitroxides or added at the time of formulation) leads to what can be called stored radical potential. Post heating of a cured film which contains these materials shows a significant increase in MEKR. The apparent activation energies of post curing, and the dependence on oxygen concentration dur-

ing cure, suggests that oxidized species, rather than alkoxyamines themselves, are responsible for releasing radicals during thermal initiation.

Acknowledgements

Patrick Kramer acknowledges the support of Sun Chemical Corporation for employment through the summer internship program in 2009, 2010, and 2011.

References

- [1] Christian Decker. Light-induced crosslinking polymerization. *Polymer International*, 51:1141–1150, 2002.
- [2] Paul C. Painter and Michael M. Coleman. *Fundamentals of Polymer Science: An Introductory Text*. Technomic, Lancaster, PA, second edition, 1997.
- [3] George Odian. *Principles of Polymerization*. Wiley-Interscience, third edition, 1991.
- [4] J. K. Fink. Determination of in-cage and out-of-cage recombination of initiator radicals in solution polymerization using labeled initiators. *Journal of Polymer Science: Polymer Chemistry Edition*, 21:1445–1455, 1983.
- [5] Athelstan L. J. Beckwith and James. S. Poole. Factors affecting the rates of addition of free radicals to alkenes—determination of absolute rate coefficients using the persistent aminoxyl method. *Journal of the American Chemical Society*, 124:9489–9497, 2002.
- [6] J. Lalevée, X. Allonas, and J. P. Fouassier. Direct measurements of the addition and recombination of acrylate radicals: Access to propagation and termination rate constants? *Journal of Polymer Science: Part A: Polymer Chemistry*, 44:3577–3587, 2006.
- [7] Dhananjay Dendukuri, Priyadarshi Panda, Ramin Haghgooie, Ju Min Kim, T. Alan Hatton, and Patrick S. Doyle. Modeling of oxygen-inhibited free radical photopolymerization in a PDMS microfluidic device. *Macromolecules*, 41:8547–8557, 2008.
- [8] Katia Studer, Christian Decker, Erich Beck, and Reinhold Schwalm. Overcoming oxygen inhibition in UV-curing of acrylate coatings by carbon dioxide inerting, part I. *Progress in Organic Coatings*, 48:92–100, 2003.
- [9] Katia Studer, Christian Decker, Erich Beck, and Reinhold Schwalm. Overcoming oxygen inhibition in UV-curing of acrylate coatings by carbon dioxide inerting, part II. *Progress in Organic Coatings*, 48:101–111, 2003.
- [10] Sindee L. Simon, Gregory B. McKenna, and Olivier Sindt. Modeling the evolution of the dynamic mechanical properties of a commercial epoxy during cure after gelation. *Journal of Applied Polymer Science*, 76:495–508, 2000.
- [11] Mario Farina. Chemistry and kinetics of the chain transfer reaction. *Makromolekulare Chemie, Macromolecular Symposia*, 10-11:255–272, 1987.
- [12] G. Moad and D. H. Solomon. *The Chemistry of Free Radical Polymerization*. Pergamon, Oxford, 1995.
- [13] Osamu Ito, Yuichi Arito, and Minoru Matsuda. Captodative effect on rates of addition reactions of arylthiyl radicals to disubstituted olefins. *Journal of the Chemical Society, Perkin Transactions 2*, pages 869–873, 1988.
- [14] Asit K. Chandra and Minh Tho Nguyen. New look at free radical addition to olefins using local reactivity indices. *Journal of the Chemical Society, Perkin Transactions 2*, pages 1415–1417, 1997.
- [15] Thomas Junkers and Christopher Barner-Kowollik. The role of mid-chain radicals in acrylate free radical polymerization: Branching and scission. *Journal of Polymer Science: Part A: Polymer Chemistry*, 46:7585–7605, 2008.
- [16] Aäron G. Vandeputte, Marie-Françoise Reyniers, and Guy B. Marin. Theoretical study of the thermal decomposition of dimethyl disulfide. *Journal of Physical Chemistry A*, 114:10531–10549, 2010.

- [17] Grażyna Wenska, Katarzyna Taras-Goślińska, Bohdan Snalski, Gordon L. Hug, Ian Carmichael, and Bronislaw Marciniak. Generation of thiyl radicals by the photolysis of 5-iodo-4-thiouridine. *Journal of Organic Chemistry*, 70:982–988, 2005.
- [18] Kathleen B. Gross, Susan C. Noe, Alphonsus V. Pocius, William J. Schultz, and Wendy L. Thompson. Adhesives and adhesive compositions containing thioether groups. US Patent 6,800,371, 3M Innovative Properties Company, 2004.
- [19] Dimitris Vlassopoulos. Colloidal star polymers: Models for studying dynamically arrested states in soft matter. *Journal of Polymer Science: Part B: Polymer Physics*, 42:2931–2941, 2004.
- [20] Igor V. Khudyakov and Nicholas J. Turro. Cage effect dynamics under photolysis of photoinitiators. *Designed Monomers and Polymers*, 13:487–496, 2010.
- [21] Jean-Pierre Fouassier. *Photoinitiation, Photopolymerization, and Photocuring: Fundamentals and Applications*. Hanser, Munich, 1995.
- [22] Igor V. Khudyakov and Nicholas J. Turro. Laser flash photolysis of photoinitiators: ESR, optical, and IR spectroscopy detection of transients. In Malcom D. Forbes, editor, *Carbon-Centered Free Radicals and Radical Cations*, chapter 12. Wiley, New York, NY, 2010.
- [23] Hubert Charles Bailey. A process for the stabilization of acrylonitrile by distillation with a nitroxide. US Patent 3,747,988, BP Chemicals Limited, 1973.
- [24] Craig J. Hawker, Anton W. Bosman, and Eva Harth. New polymer synthesis by nitroxide mediated living radical polymerizations. *Chemical Reviews*, 101:3661–3688, 2001.
- [25] Jeremy R. Lizotte. *Synthesis and Characterization of Tailored Macromolecules via Stable Free Radical Polymerization Methodologies*. PhD thesis, Virginia Polytechnic Institute and State University, Blacksburg, Virginia, August 2003.
- [26] D. R. Bauer. Kinetics of photooxidation and photostabilization in crosslinked polymer coatings. *Polymer Degradation and Stability*, 48:259–267, 1995.
- [27] Jennifer L. Hodgson and Michell L. Coote. Clarifying the mechanism of the denisov cycle: How do hindered amine light stabilizers protect polymer coatings from photo-oxidative degradation? *Macromolecules*, 43:4573–4583, 2010.
- [28] Jennifer L. Hodgson, Luke B. Roskop, Mark S. Gordon, Ching Yeh Lin, and Michelle L. Coote. Side reactions of nitroxide-mediated polymerization: N–O versus O–C cleavage of alkoxyamines. *Journal of Physical Chemistry A*, 114:10458–10466, 2010.
- [29] Atsushi Goto and Takeshi Fukuda. Comparative study on activation rate constants for some styrene/nitroxide systems. *Macromolecular Chemistry and Physics*, 201:2138–2142, 2000.
- [30] Sylvain Marque, Hanns Fischer, Elisabeth Baier, and Armido Studer. Factors influencing the C–O bond homolysis of alkoxyamines: Effects of H-bonding and polar substituents. *Journal of Organic Chemistry*, 66:1146–1156, 2001.
- [31] Peter P. Klemchuk and Matthew E. Gande. Stabilization mechanisms of hindered amines. *Polymer Degradation and Stability*, 22:241–274, 1988.
- [32] Peter P. Klemchuk, Matthew E. Gande, and Enzo Cordola. Hindered amine mechanisms: Part III—investigations using isotopic labelling. *Polymer Degradation and Stability*, 27:65–74, 1990.
- [33] Eugene N. Step, Nicholas J. Turro, Matthew E. Gande, and Peter P. Klemchuk. Mechanism of polymer stabilization by hindered-amine light stabilizers (HALS). model investigations of the interaction of peroxy radicals with HALS amines and amino ethers. *Macromolecules*, 27:2529–2539, 1994.
- [34] Eugene N. Step, Nicholas J. Turro, Peter P. Klemchuk, and Matthew E. Gande. Model studies on the mechanism of HALS stabilization. *Die Angewandte Makromolekulare Chemie*, 232:65–83, 1995.
- [35] Arthur A. Frost and Ralph G. Pearson. *Kinetics and Mechanism: A Study of Homogenous Chemical Reactions*. John Wiley & Sons, Inc., second edition, 1961.